Available online at www.sciencedirect.com
SCIENCE DIRECT
Polymer 46 (2005) 4853–4867
polymer
www.elsevier.com/locate/polymer

Formation of water-resistant hyaluronic acid nanofibers by blowing-assisted electro-spinning and non-toxic post treatments

Xuefen Wang[a], In Chul Um[a], Dufei Fang[b], Akio Okamoto[c], Benjamin S. Hsiao[a], Benjamin Chu[a,*]

[a]*Department of Chemistry, Stony Brook University, Stony Brook, NY 11794-3400, USA*
[b]*Stonybrook Technology and Applied Research Inc., P.O. Box 1336, Stony Brook, NY 11790, USA*
[c]*Denka Research Center, 3-5-1 Asahimachi, Machida, Tokyo 194-8560, Japan*

Received 29 November 2004; received in revised form 11 March 2005; accepted 14 March 2005
Available online 3 May 2005

Abstract

A unique blowing-assisted electro-spinning process has been demonstrated recently to fabricate hyaluronic acid (HA) nanofibers. In this article, effects of various experimental parameters, such as air-blowing rate, HA concentration, feeding rate of HA solution, applied electric field, and type of collector on the performance of blowing-assisted electro-spinning of HA solution were investigated. With the assistance of air-blowing, the solution-feeding rate could be increased to 40 μl/min/spinneret and the applied electric field could be decreased to 2.5 kV/cm. The optimum conditions for consistent fabrication of HA (with a molecular weight of ~3.5 million) nanofibers involved the use of an air-blowing rate of around 70 ft^3/h and a concentration range between 2.5 and 2.7% (w/v) in aqueous solution. Two benign methods to fabricate water-resistant HA nanofibrous membranes without the use of reactive chemical agents were demonstrated: (a) the exposure of HA membranes in hydrochloric acid (HCl) vapor, followed by a freezing treatment at −20 °C for 20–40 days; and (b) the immersion of HA membranes in an acidic mixture of ethanol/HCl/H_2O at 4 °C for 1–2 days. Although both methods could produce hydrophilic, substantially water-resistant HA nanofibrous membranes (the treated membranes could keep their shape intact in neutral water at 25 °C for about 1 week), the immersion method (6) was shown to be more versatile and effective. IR spectroscopy was used to investigate this 'cross-linking' mechanism in the solid HA membrane. Viscosity studies of acidic HA solutions under varying freezing conditions were also carried out. It was found that when the freezing time exceeded 8 h, the HA solution became gel-like and exhibited a large increase in the hydrogen-bond concentration. Thus, the resistance to water solubility could be due to the high density of hydrogen bonds in the solid HA membranes that were treated by the 'freezing' approach.

Keywords: Hyaluronic acid; Electro-spinning; Air-blowing

1. Introduction

Electro-spun nanofibrous membranes exhibit many potential applications, including tissue engineering, drug delivery, filtration, protective clothing, sensors, etc. [1–8]. The electro-spinning process is relatively complex because of the many controlling and coupled parameters, such as applied electric field, solution feeding rate, solvent evaporation rate, polymer solution concentration, degree of molecular entanglement in solution, etc. [9–14]. To date, it is believed that nearly one hundred different polymers have been successfully electro-spun [15]. However, there are many more polymers that could not be electro-spun successfully. One of them is the hyaluronic acid (HA), a naturally occurring polysaccharide, commonly found in connective tissues in the body such as vitreous, umbilical cord, and joint fluid, due to its very high solution viscosity and high surface tension, even at fairly low solution concentrations. HA is a polyanionic acid that has unique physicochemical properties and distinctive biological functions. Its unusually high viscosity at low concentrations and room temperatures has been utilized for surgical treatments in ophthalmology as a viscoelastic biomaterial protecting ocular cells from damage during surgery [16–22]. The

* Corresponding author. Tel.: +1 631 632 7928; fax: +1 631 632 6518.
E-mail address: bchu@notes.cc.sunysb.edu (B. Chu).

0032-3861/$ - see front matter © 2005 Elsevier Ltd. All rights reserved.
doi:10.1016/j.polymer.2005.03.058

chemical structure of HA, consisting of repeated disaccharide units of D-glucuronic acid and N-acetyl-D-glucosamine, is illustrated as follows.

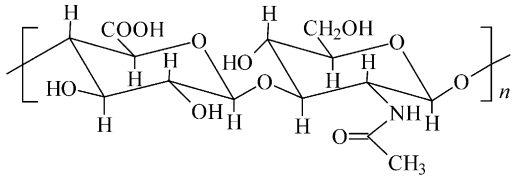

Recently, we have successfully demonstrated the fabrication of HA nanofibers using the blowing-assisted electro-spinning technique (we previously termed it 'electro-blowing'), which combined the process of electro-spinning with air-blowing capability around the spinneret [23]. We demonstrated that there are at least four advantages in the blowing-assisted electro-spinning process. (1) The combination of air-blowing force and the applied electric field is capable of overcoming the high viscosity, as well as the high surface tension, of the polymer solution. (2) The use of an appropriate elevated temperature of the blown air can further decrease the HA solution viscosity at the spinneret, facilitating the jet formation of the HA solution at the spinneret. (3) The blowing air can accelerate the solvent evaporation process, a necessary condition for the fiber formation before the jet reaches the ground collector during the process. (4) The fiber diameter, which is one of the key factors to control the physical properties of nanofibrous membranes, can be tailored by controlling the air temperature, the direction of air-flow, and the air flowing rate. With these advantages, it is expected that many useful polymers, which could not be electro-spun before, can now be processed by using the new blowing-assisted electro-spinning approach. Furthermore, the blowing-assisted electro-spinning process shall increase the production rate and thus can lead toward more practical mass production schemes.

Although our early study demonstrated the successful fabrication of nanofibrous HA membranes by blowing-assisted electro-spinning [23], the efficiency of nanofiber production with consistency and uniform diameter output in the range of 100 nm was relatively low. In order to produce better quality HA nanofibrous membranes and higher throughput, the first part of this study is devoted to the investigation of several key parameters in blowing-assisted electro-spinning, which includes the air-blowing rate, HA solution concentration, feeding rate of HA solution, applied electric field, and type of collectors, on the fabrication of uniform HA nanofibers. The second part of this study aims to resolve the following problem. The electro-spun HA nanofibrous membranes, due to the very large surface-to-volume ratios, dissolve instantly in water. As a result, an effective post-processing procedure must be developed to treat hydrophilic electro-spun HA membranes in order to make them water-resistant. For biomedical applications, it is also preferred not to use additional chemicals for the cross-linking process.

In the past, many attempts have been made to introduce cross-linking sites into HA molecules to produce insoluble or gel-like HA materials. The chemical cross-linking reagents used in previous studies included diepoxy [24], glutaraldehyde [25], carbodiimide [26,27] and disulfide [28]. Unfortunately, conventional chemical modifications and subsequent cross-linking of HA have an inevitable problem of extra risks, such as toxicity and bio-incompatibility, intrinsic to most chemical modifications. To the best of our knowledge, there is only one physical method for making 'insoluble' or 'water resistant' HA gels, which involves simultaneous freezing and thawing of acidic aqueous HA solution [29]. Some physical pathways, which were inspired by this method of using only non-toxic agents to generate water-resistant HA, were also investigated in this study to produce water-resistant nanofibrous HA membranes. Two criteria were set for the successful preparation of these membranes: (1) the nanofibrous texture in the post-processed electro-spun HA membrane should remain intact after the treatment; (2) the post-processed HA membrane should remain insoluble in water for about 1 week, a time period that is sufficiently long for specific applications in the prevention of post-operative induced adhesions as well as in tissue engineering [30].

2. Experimental

2.1. Preparation of HA solution

The HA solution for blowing-assisted electro-spinning was prepared using the same method as reported in our previous paper [23]. High molecular weight HA (with a weight average molecular weight, M_w, of about 3.5 million g/mol), extracted from the culture broth *Streptococcus equi*, was supplied by Denki Kagaku Kogyo Co. Ltd (Japan). The HA powder sample was dissolved in an acidic aqueous solution (pH = 1.5) by stirring. Upon the formation of homogeneous HA solution, the sample was moved to the syringe pump for solution delivery in the blowing-assisted electro-spinning process.

2.2. Blowing-assisted electro-spinning of HA nanofibrous membranes

The same blowing-assisted electro-spinning apparatus introduced in our previous paper [23] was used for this study (a schematic diagram of this apparatus is shown in Fig. 1). The air-blowing rate ranged from 35 to 150 ft^3/h. The HA concentration ranged from 2.0 to 3.0% (w/v). The solution-feeding rate was varied in the range of 20–60 μl/min. The applied electric field ranged from 25 to 40 kV and the distance between the spinneret and the ground collector was set at 9.5 cm. The blowing rate and the temperature of

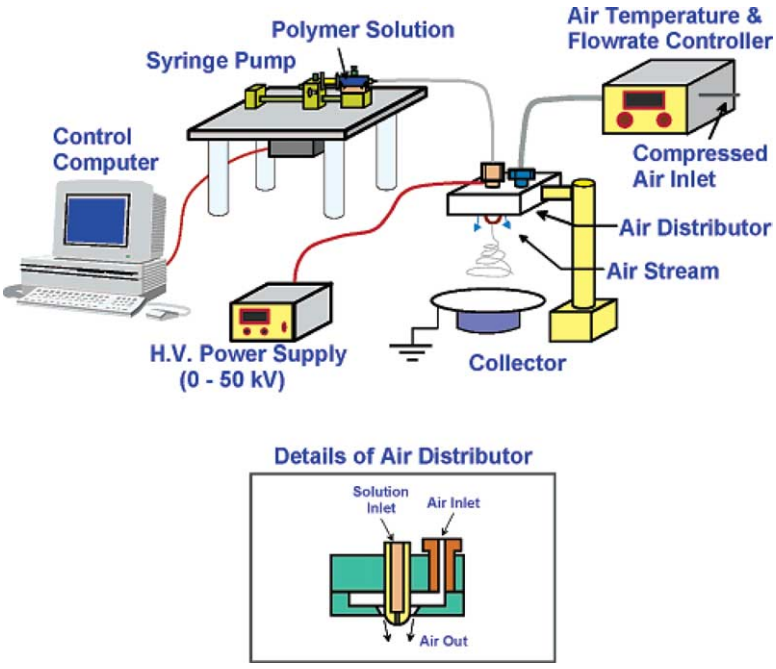

Fig. 1. Scheme diagram for electro-spinning and electro-blowing setup used in this study (figure is reproduced from Ref. [23] with permission).

air-blowing could be varied within a precision of about 2% and $\pm 2°$, respectively. To examine the effects of the type of collectors on the performance of blowing-assisted electro-spinning, three different types of collectors were tested: aluminum foil, wire screen, and wire screen on aluminum foil. For the wire screen, different hole sizes, 1.7 and 6.3 mm, and different collection times, 20 and 40 min, were used to investigate the effects of collection area and collection time on the blowing-assisted electro-spinning performance of HA solution.

2.3. Post-treatments to fabricate water resistant electro-spun HA nanofibrous membranes

Two post-treatment processes, similar to the method described by Miyata et al. [29], were first tested on the cast HA films, prepared from a 1.5% (w/v) acidic aqueous HA solution using the following procedures. The HA solution was cast on a clean glass plate and subsequently dried at 25 °C for 3 days. The thickness of the cast HA film was about 20 μm. The optimized conditions for these two post-treatments were then applied to electro-spun HA nanofibrous membranes of similar (bulk) thickness.

2.3.1. HCl-vapor treatment

A cast HA film or an electro-spun HA membrane was pasted on the inner surface of a petri dish, which was placed on the top of a beaker containing 10-ml hydrochloride acid (HCl) aqueous solution at varying concentrations (20–37% (w/v)). After several minutes (up to 10 min.) of HCl-vapor treatment, the film/membrane was taken out, sealed in a bottle, and placed in a freezer at -20 °C for different periods of time (20–40 days).

2.3.2. Solution treatment by acidic alcohol/water mixture

The HA sample (a cast film or an electro-spun membrane) was directly immersed in a three-component mixture, containing varying ratios of ethanol, water and 37% (w/v) HCl, with the percent of HCl being based on water as 100% for different amounts of time (in the range of days) and at different temperatures (-20 to 20 °C). Ethanol was chosen because it is a non-solvent for HA and it is completely miscible with water. In addition, it is considered relatively 'non-toxic' for biomedical applications.

2.4. Sample characterizations

The key virtue of the above post-treatment process utilized essentially only water, an acid and/or ethanol, which were subsequently washed away upon the recovery of the final samples. No additional chemicals of any kind were involved in the cross-linking procedures.

The shear viscosity of the HA solution was measured by using a rheometrics mechanical spectrometer (RMS-605E, Rheometrics, Inc., USA) to investigate the effect of viscosity on the performance of the blowing-assisted electro-spinning process. The 50 mm plate–plate geometry was utilized for rheological measurements. The shear rate was changed from 1 to 1000 s^{-1} and the measurements were performed at 25, 39, 47, and 57 °C, respectively.

The surface of as-spun or post-treated electro-spun HA membranes was characterized by scanning electron microscopy (SEM) (LEO1550, LEO, USA) to evaluate the

effects of different processing parameters on the blowing-assisted electro-spinning performance of HA solution. The fiber diameters were determined from the SEM micrographs by using a custom code image analysis program, where the average value was obtained from measurements of 50 different fibers in the electro-spun HA membrane.

To explore the possible mechanism of the 'cross-linking' process of HA membrane and solution under acidic conditions, the following experiments were also carried out. The HA powder was dissolved in Mill-Q water to prepare a 1–2% (w/v) HA aqueous solution, where the pH level of the solution was adjusted to 1.5 using 0.1 N HCl. This acidic solution was frozen at −20 °C over different time periods (0–3, 6, 8, 10, 40 h) and then thawed at 25 °C. A 40-h freezing period was used as a reference point, which yielded a spongy HA gel. Shear viscosity measurements of acidic HA solutions that had been frozen for different time periods were performed on the RMS 605E at room temperatures using a parallel plate (50 mm diameter) fixture. The intrinsic viscosity of diluted HA solution after freezing was measured by using a Ubbelohde capillary viscometer at 25 °C. FT-IR spectra of the electro-spun membranes before and after cross-linking were measured using a Nicolet 760 spectrometer.

3. Results and discussion

3.1. Processing effects on the performance of blowing-assisted electro-spinning

3.1.1. Effect of air-blowing rate

As revealed in the previous article [23], the air-blowing rate had an important role in changing the blowing-assisted electro-spinning performance of HA solution. In the case of air-blowing at room temperatures, although the electro-spinning performance was improved by an increase in the blowing rate, it did not allow the persistent production of nanofibers, due mainly to the limited change in the evaporation rate of solvent when the room temperature air was employed. Therefore, in this study, we used hot air and investigated the effects of air-blowing rate at higher temperatures on the electro-spinning performance. Fig. 2 shows the morphological changes of electro-spun HA fibers by controlling the air-blowing rate. When the air-blowing rate was increased to 70 ft^3/h, the bead formation was found to be minimized. However, a further increase in the air-blowing rate somewhat deteriorated the nanofiber formation process, implying the existence of an optimal condition for successful blowing-assisted electro-spinning of HA solution

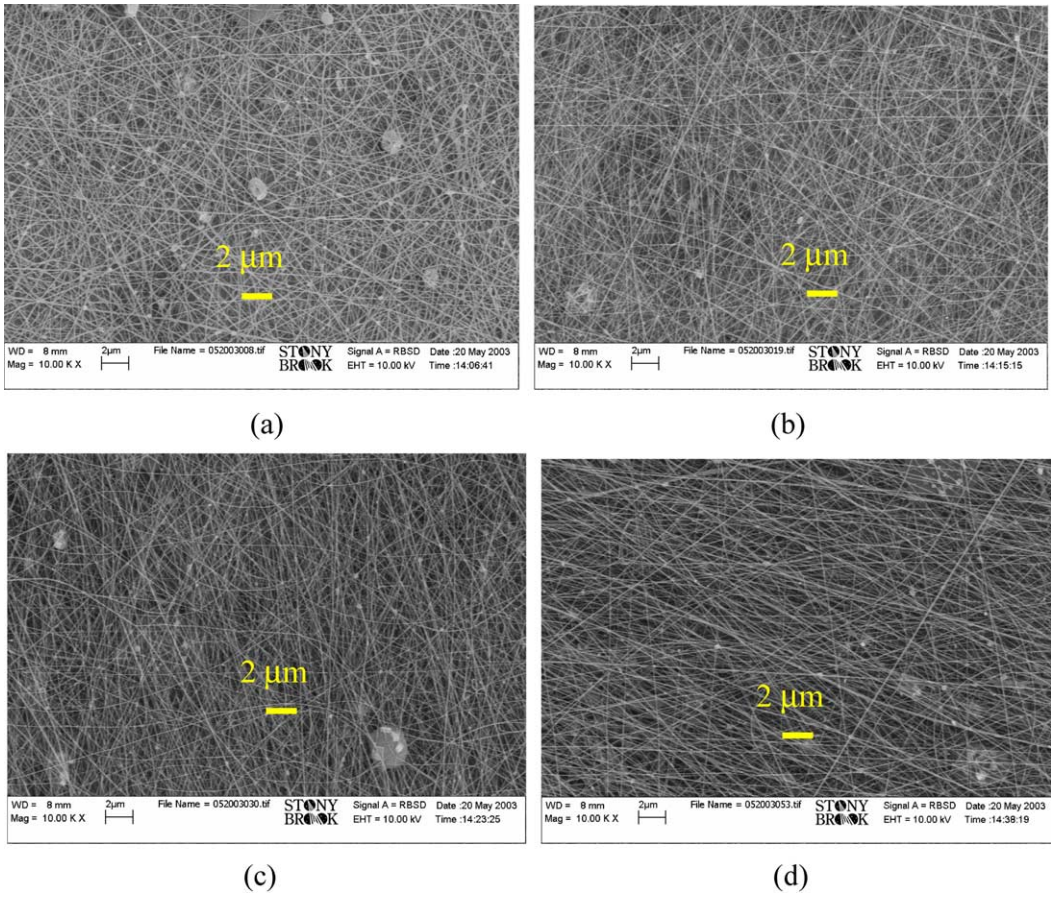

Fig. 2. Effect of air-blowing rate on the morphology of HA nanofibers from 2.5% (w/v) HA solution; (a) 35 ft^3/h (61 °C), (b) 70 ft^3/h (57 °C), (c) 100 ft^3/h (55 °C), (d) 150 ft^3/h (56 °C).

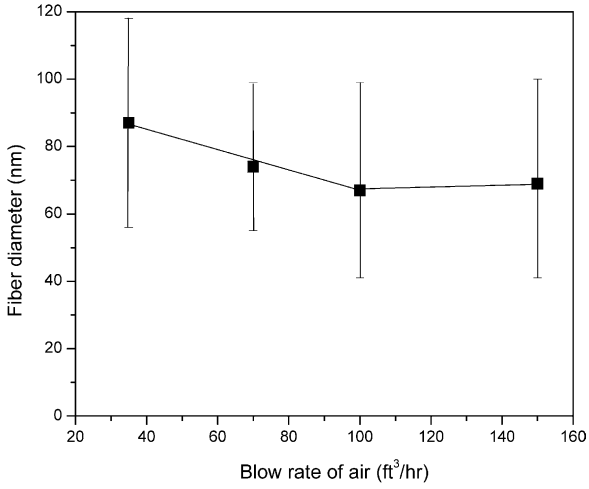

Fig. 3. Effect of blow rate of air on the diameter of HA nanofibers electro-spun from 2.5% (w/v) HA solution.

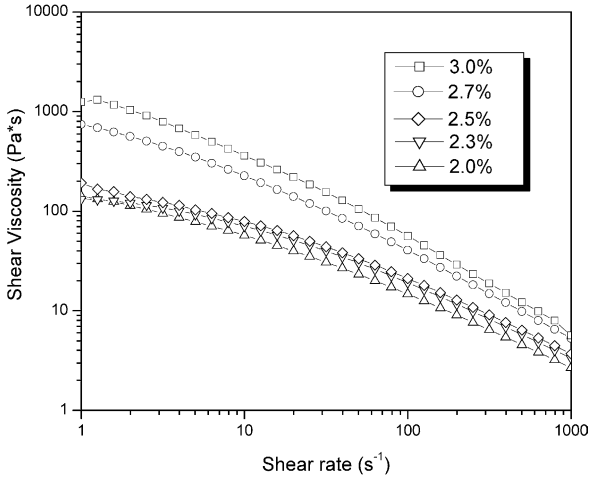

Fig. 4. Shear viscosity of HA solutions with various concentrations (%(w/v)) at 57 °C.

using the existing geometry of our current setup. In Fig. 2, it is seen that temperature also affects the blowing-assisted electro-spinning process. However, we could conclude that this effect was minor in the chosen operating conditions because the rate of 35 ft^3/h, at a higher temperature (61 °C), showed less distinct fiber morphology than the rate of 70 ft^3/h at 57 °C. The temperature variation at different temperatures was due to the difficulty in controlling the air temperature when the air-flowing rate became high.

It seems that the air-blowing rate at high temperatures has a positive effect—a fast evaporation rate, as well as a negative effect—a rapid viscosity increase due to the concentration increase, on the blowing-assisted electro-spinning process. It is conceivable that the effect due to an increase in the drying rate is the predominant factor below the air-blow rate of 70 ft^3/h. At a rate above 70 ft^3/h, the rapid viscosity rise due to faster drying becomes unfavorable to the blowing-assisted electro-spinning process, resulting in a decrease in the membrane quality. We noted that the blowing-assisted electro-spinning performance was improved with increasing air-blow rate at room temperatures because a slower solvent evaporation rate could be related to the air-blowing at room temperatures.

The diameter of electro-spun HA fibers resulting from different air-blowing rates is shown in Fig. 3. With an increase in the air-blowing rate (less than 100 ft^3/h), the fiber diameter was found to decrease. Above the rate of 100 ft^3/h, no further change of the fiber diameter was observed. This observation can be explained as follows. The increase in the air-blowing rate can lead to an increase in the solvent evaporation rate and consequently enhance the HA polymer chain stretching during the blowing-assisted electro-spinning process, because the entangled polymer chains at higher concentrations could be stretched further during the elongation process. However, if the concentration increase becomes too fast (at a more rapid evaporation rate), the chain stretching process may not take place effectively, resulting in a reduction in the spin-draw ratio and an increase in the fiber diameter. Thus, the air-blowing rate at high temperatures can have multiple implications in controlling the fiber formation. It is assumed that the elongation effect by air-blowing is predominant at the blowing rate below 100 ft^3/h at about 60 °C. After that rate, the effect of chain extension is hindered by the faster evaporation rate leading to no further reduction in the fiber diameter.

3.1.2. Effect of HA concentration

Polymer concentration has been known as one of the key parameters in electro-spinning [31] because it determines the solution viscosity, the polymer chain entanglements that are essential for successful operation and the amount of solvent that must be removed in the electro-spinning process. The solution concentration also plays an important role in blowing-assisted electro-spinning. SEM results of

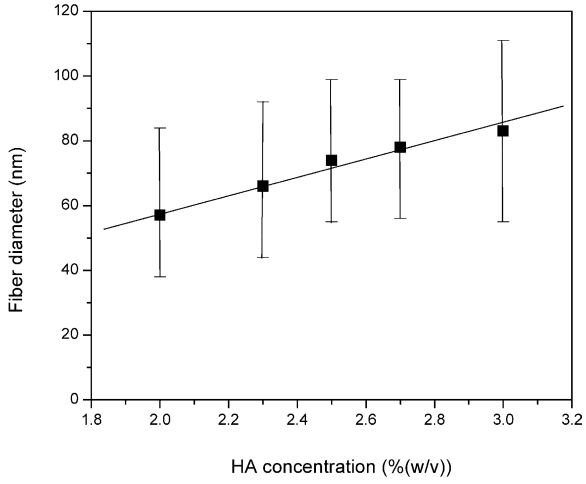

Fig. 5. Effect of HA concentration on HA fiber diameter by using the blowing-assisted electro-spinning process at 57 °C of air with 70 ft^3/h of blow rate.

electro-spun HA mats (not shown here) prepared at 57 °C, 70 ft^3/h illustrated uniform fibrous morphology over a narrow concentration range from 2.5 to 2.7% (w/v), which appeared to be an optimal concentration range for blowing-assisted electro-spinning of HA at the chosen conditions. At higher solution concentrations, the electric force could not overcome the high viscosity and the surface tension of the fluid, resulting in the failure to produce a stable jet stream. On the other hand, at low concentrations, the polymer chains are not sufficiently entangled to form fibrous morphology. Thus, the combination of air-blowing and electrical force increases the boundary conditions acceptable for polymer solutions within a viscosity, surface tension, concentration, and molecular weight range. The optimum concentration range (2.5–2.7% (w/v)) for blowing-assisted electro-spinning of HA of the given molecular weight at 57 °C and 70 ft^3/h corresponds to a viscosity range from 200 to 800 Pa s, which is shown in Fig. 4. In our previous report, the optimal viscosity range for blowing-assisted electro-spinning of HA solution at room temperature was 3–30 Pa s. This suggests that the increase in temperature effectively increases the viscosity range of the solution that can be electro-spun.

With the increase in solution concentration, the average fiber diameter of electro-spun fibers was found to increase from 57 to 83 nm, which is shown in Fig. 5. The relationship between fiber diameter and polymer concentration has been reported by us earlier [14]. As a smaller amount of the solvent at higher polymer concentrations needs to be removed in a fixed time period, the faster evaporation of the solvent at higher concentrations could reduce the spin-draw ratio during blowing-assisted electro-spinning, resulting in a larger fiber diameter. It is interesting to note that the blowing-assisted electro-spun HA fiber exhibits a smaller diameter than that of polymer samples (other than HA) prepared by the conventional electro-spinning technique. This may be due to two reasons. The first reason is related to the lower HA concentration we used in the blowing-assisted electro-spinning process. As seen in Fig. 5, the diameter of electro-spun fiber was increased with an increase in solution concentration. Therefore, it is conceivable that the production of smaller size fibers resulted from the lower HA concentration. In general, a low concentration of around 2% (w/v) is not easily electro-spun due to low viscosity, less polymer chain entanglement, and high solvent amount; therefore it is not easy to produce small fiber diameters simply by reducing the polymer concentration. The second reason is due to the high spin-draw ratio during our blowing-assisted electro-spinning process. It is found that our blowing-assisted electro-spinning system can generate a higher spin-draw ratio than the conventional electro-spinning system since the effective pulling force can be enhanced by a combination of electric field and air-blowing.

3.1.3. Effect of solution feeding rate

The feeding rate of solution during blowing-assisted electro-spinning is another factor affecting the fabrication process including electro-spinnability [31], yield efficiency, and fiber diameter. In this study, 2.5% (w/v) HA solution was electro-spun by using different fluid feeding rates in order to elucidate their effects on the process. By using SEM to evaluate the performance of the final sample, the optimal feeding rate was from 20 to 60 μl/min. Above 60 μl/min, an unstable jet was developed abruptly. Thus, in our current study, the optimum feeding rate was set to be 40 μl/min, in order to maintain the jet stability and to increase the production efficiency. We noted that the optimum feeding rate for electro-spinning of HA at room temperature was 5–10 μl/min, while the range of feeding rate for blowing-assisted electro-spinning at 60 °C could be much higher (20–60 μl/min). In a typical electro-spinning operation, there is a narrow window of feeding rate for successful processing because the consumption of solution being electro-spun has to be limited to within a certain range in order to maintain the Taylor cone at the spinneret. When the solution-feeding rate is lower than this range, the Taylor cone can be broken. When the solution-feeding rate is higher than this range, the extra solution will drip out, which can interfere with the electro-spinning process. For blowing-assisted electro-spinning, the added parameter is the introduction of air-blowing. As mentioned earlier, the air-blowing has two major effects on the spinning process: (1) an increase in the evaporation rate and (2) an enhancement in the effective fiber pulling force. We believe that in the chosen study to demonstrate the broadened capability of blowing-assisted electro-spinning, the effect of increasing evaporation rate is one of the dominant factors because the faster evaporation rate by air-blowing will make the solution around the spinneret dry faster. An increase in the solution-feeding rate is needed in order to maintain the Taylor cone, as a lower solution-feeding rate will result in the solidification of the solution during spinning [14]. The fiber diameter

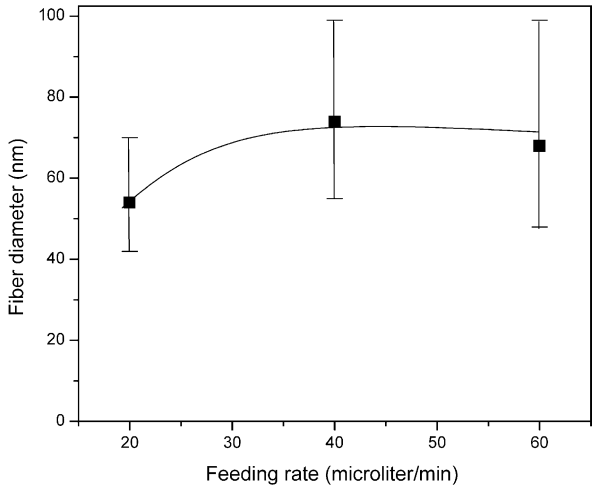

Fig. 6. Effect of solution feeding rate on the diameter of electro-spun HA fibers. The concentration, air temperature, and air-blowing rate were 2.5% (w/v), 57 °C, and 70 ft^3/h, respectively.

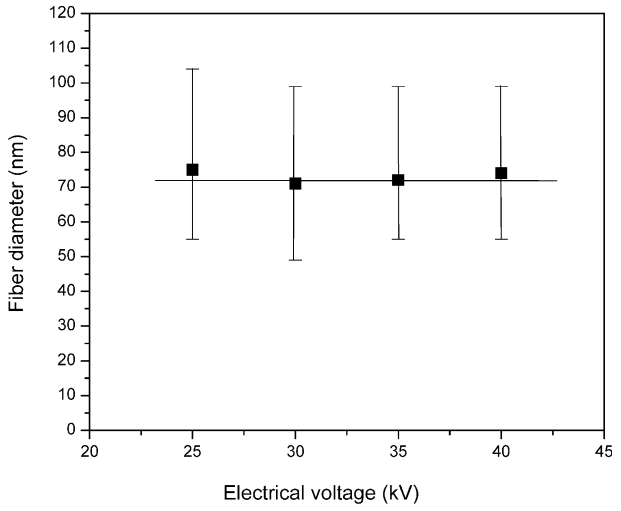

Fig. 7. Effect of electric field on the diameter of HA nanofiber electro-spun from 2.5% (w/v) solution. The air temperature and the air-blowing rate were 57 °C and 70 ft^3/h, respectively.

of electro-spun HA (from SEM images) was measured to examine the effect of feeding rate on the fiber diameter, as shown in Fig. 6. It was seen that the fiber diameter increased with increasing solution-feeding rate up to 40 μl/min, above which the fiber diameter remained nearly unchanged.

3.1.4. Effect of electric field

The applied electric field has also been known to be one of the most important factors influencing the electro-spinning process. We demonstrated that even with 40 kV of applied electric field, the HA solution could still not be electro-spun without the assistance of air due to the high viscosity of HA solution. However, the implementation of air-blowing significantly facilitates the spinning process by changing the solvent evaporation rate and by adding an extra pulling force. Results for the effect of electric field on the blowing-assisted electro-spinning performance for HA solution are shown in Fig. 7. The electric force could not overcome the surface tension until the applied electric potential reached beyond 24 kV. The jet became stabilized at 25 kV and remained stabilized until 40 kV. Above 40 kV, the blowing-assisted electro-spinning process became unstable because of the sporadic electro-static discharge from the humidity in the atmosphere. However, the measurements of fiber diameters suggested that the electric field strength in blowing-assisted electro-spinning could not significantly influence the fiber diameter, which is quite different from conventional electro-spinning [32].

3.1.5. Effect of collector type

Thus far, aluminum foil has been used as one of the most popular collectors in electro-spinning. However, it is well known that different types of collectors can result in different electro-spinnability or the resulting fiber morphology. The different collectors include wire screen, conducting cloth and conducting paper. Typically, when HA is electro-spun on the aluminum foil, it is difficult to separate the membrane from the collector. Since the wire screen allows an easier separation between the collector and the electro-spun membrane, we used wire screen as a base collector for blowing-assisted electro-spinning of HA and investigated the effect of configuration (e.g. hole size) on the blowing-assisted electro-spinning performance of HA.

Although blowing-assisted electro-spinning of HA on the wire screen collector showed good overall fiber formation, some beads were still observed in the SEM image (Fig. 8(a)), implying that the blowing-assisted electro-spinning performance using the wire screen collector was not as consistent as that using the aluminum foil (Fig. 2). With an increase in the collection time (40 min, Fig. 8(b)), the performance became worse with more bead formation. This can be explained as follows. As the surface area of the collector is decreased (wire collector), the actual electrical force (per area) between the spinneret and the collector may also be reduced, resulting in a change in blowing-assisted electro-spinning performance. In addition, with increasing collection time, more fibers are accumulated on the collector, making the wire screen less conductive and leading to a decrease in the electric force between the spinneret and the collector. To check the validity of this hypothesis, we carried out blowing-assisted electro-spinning of HA solution using a wire screen with a larger hole size and a smaller 'wire' surface area. Our hypothesis was partially confirmed since no fiber was formed on the collector (Fig. 8(c)), indicating that a smaller collection area has a negative effect on the blowing-assisted electro-spinning performance.

Another major difference between the aluminum foil collector and the wire screen collector was the permeability of air flow. Using the aluminum foil as the collector, air-blowing will experience a hindrance imposed by the collector, and the reflected air stream can interfere with the descending airflow. Such a complication could be substantially reduced with the wire screen collector since the air could permeate, at least partially, through the collector during the beginning of the process before the fibers substantially covered the screen. Therefore, we used a combination of aluminum foil and wire screen as a collector to elucidate the effect of permeability of the collector on the blowing-assisted electro-spinning performance. As shown in Fig. 8(d), the blowing-assisted electro-spinning performance of HA solution became worse when the wire screen attached with aluminum foil was used as the collector.

Several features of different collectors on the blowing-assisted electro-spinning performance could be derived. First, we can compare the two air impermeable collectors: aluminum foil (Fig. 2) and wire screen on aluminum foil (Fig. 8(d)). The aluminum foil collector, which had a larger conductive area, showed a better performance than the wire screen on the aluminum foil collector. This verified our hypothesis that a smaller conductive area of the collector had a negative effect on the performance of blowing-assisted electro-spinning. Second, we could

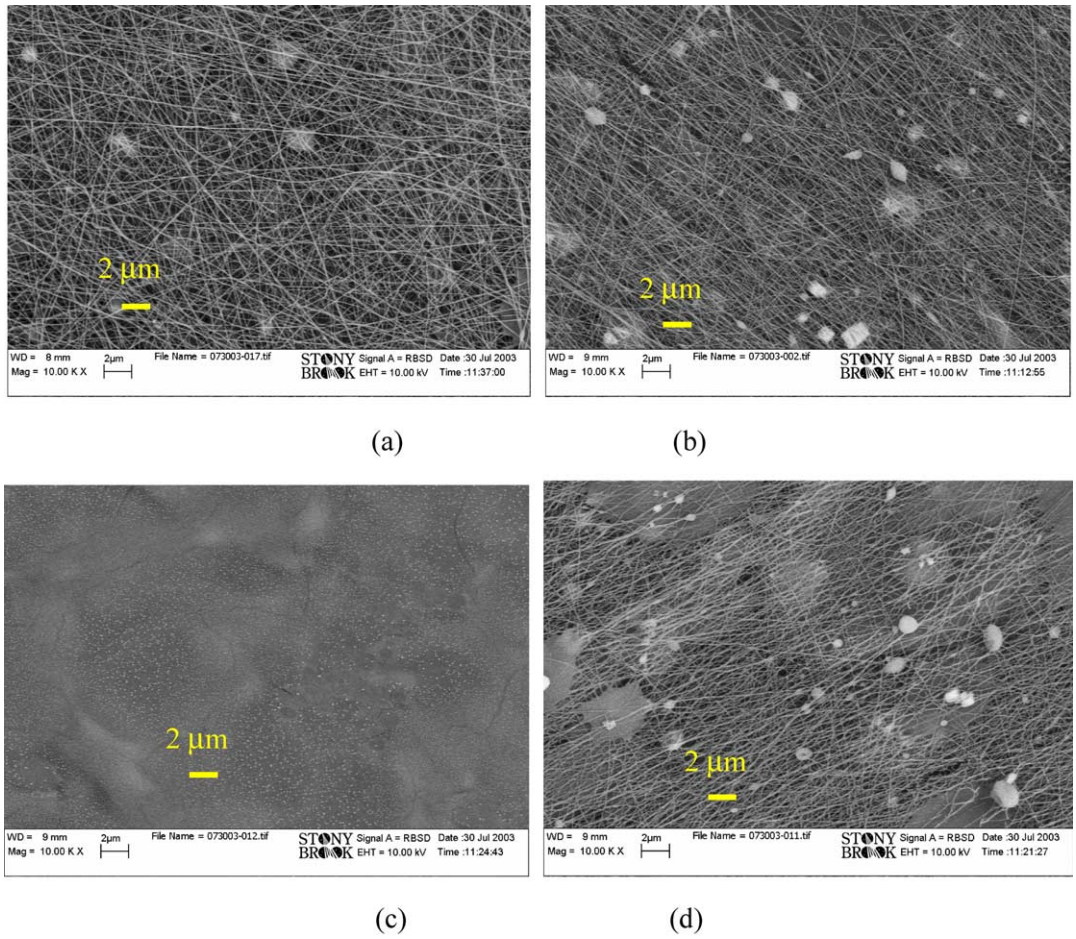

Fig. 8. Effect of type of collector used and collection time on blowing-assisted electro-spinning of HA solution: (a) wire screen (20 min, 1.7 mm of hole size), (b) wire screen (40 min, 1.7 mm hole size), (c) wire screen (40 min, 6.3 mm hole size), and (d) wire screen (40 min, 1.7 mm hole size) on aluminum foil.

compare the performance from the collectors of the same conductive area but different air permeability; wire screen with (Fig. 8(d)) and without aluminum foil (Fig. 8(b)). The pure wire screen collector with good air permeability showed much better consistency on fiber formation.

Measurements of electro-spun HA fiber diameters were also informative in achieving a better understanding of the blowing-assisted electro-spinning process. A comparison between the air permeable and impermeable collectors indicated that the air permeable collector (wire screen) produced finer fibers, perhaps due to the fact that the air permeable collector allowed a stronger air-flow, resulting in thinner fiber formation. In contrast, in the case of impermeable collectors, as the collector generated reflected air it could interfere with the descending air stream, resulting in lower spin draw ratio. It is also interesting to note that the air permeable collector can generate fibers with a narrower variation in size distribution, when compared with that from the impermeable collector, probably because of more homogeneous air-flowing streams for the air permeable collector. If there were interferences between the descending air stream and the reflected air stream, an inhomogeneous air environment could be generated, resulting in a broader degree of size distribution in the fiber diameter.

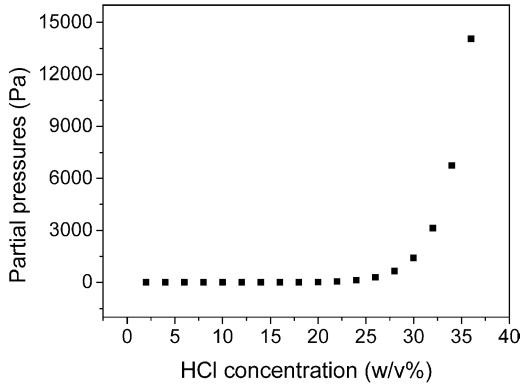

Fig. 9. Partial pressure of aqueous HCl solutions as a function of HCl concentration at 20 °C [33].

3.2. Post-treatments to produce water resistant electro-spun nanofibrous HA membranes

3.2.1. HCl-vapor treatment

The method to produce water-'insoluble' HA gels by

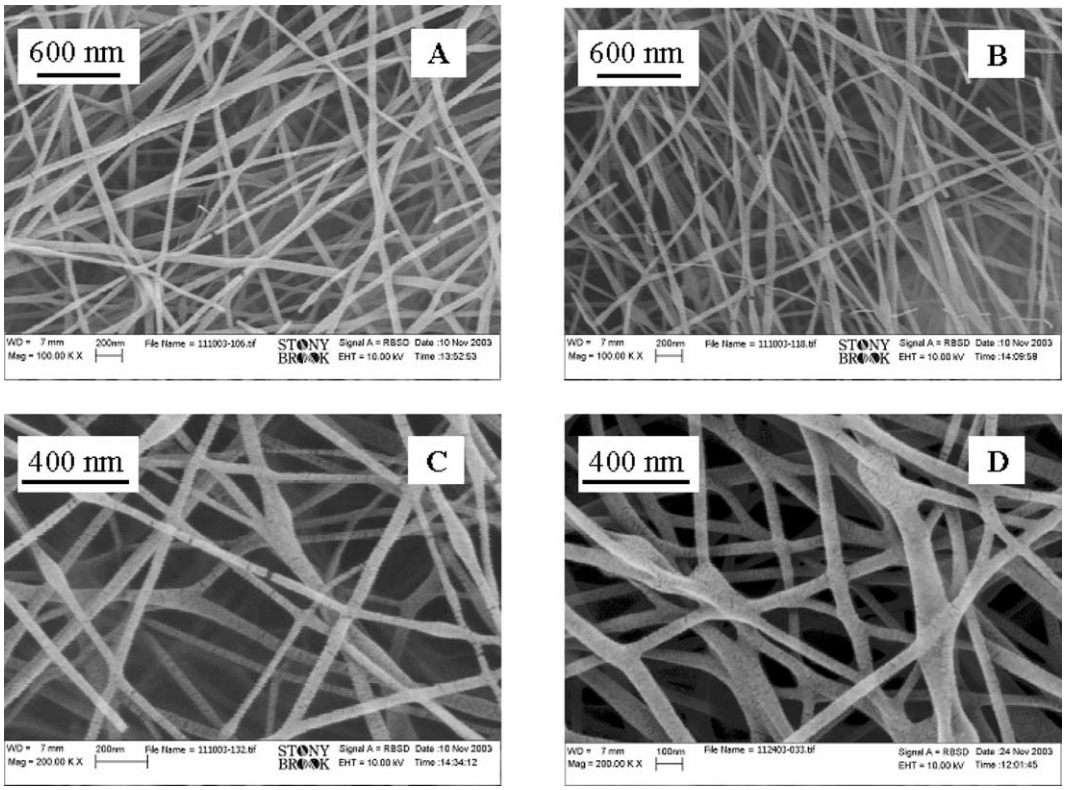

Fig. 10. SEM images of electro-spun HA membranes treated with HCl vapor for 3 min (height: 5 cm from HCl solution) from HCl aqueous solutions at different HCl concentrations: (A) 29, (B) 24, (C) 20, (D) 26% (w/v).

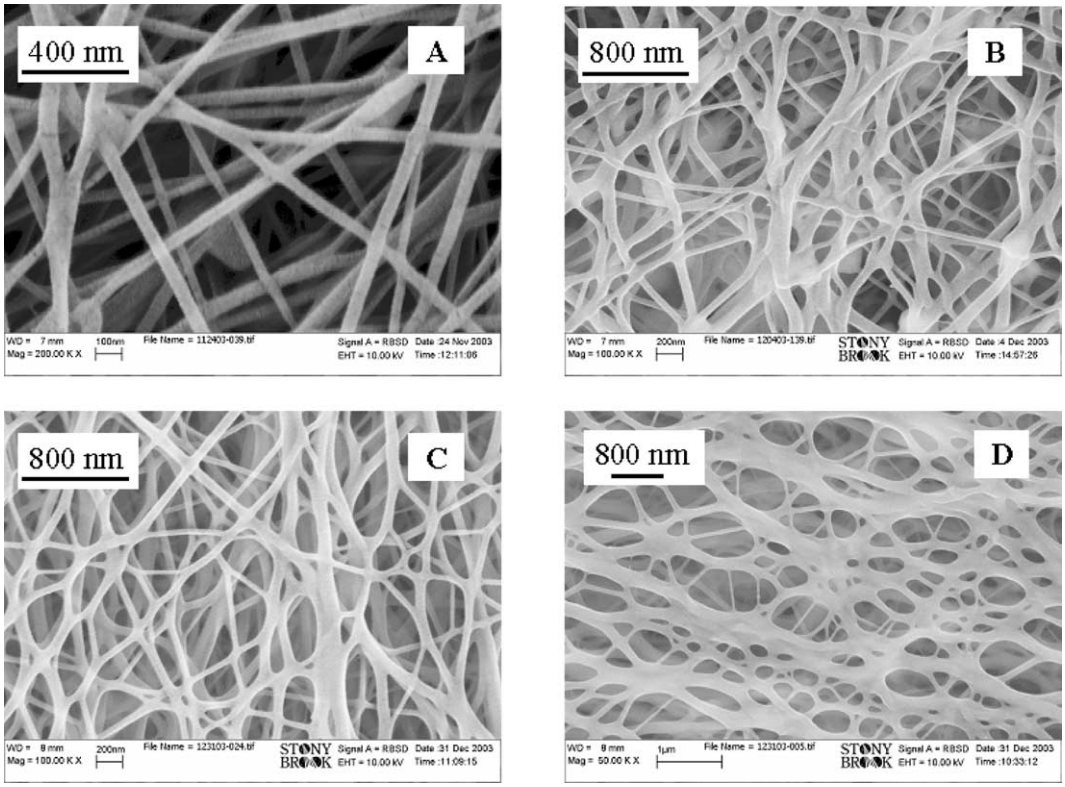

Fig. 11. SEM images of electro-spun HA membranes treated with HCl vapor from 26% (w/v) HCl aqueous solution (height: 8 cm—membrane at about 8 cm from the liquid surface) for 10 min (A, B, and C) and 25 min (D), then kept at −20 °C for: (A) 0 day; (B) 10 days; (C) 35 days; (D) 35 days.

freezing and thawing acidic aqueous solutions (pH ~ 1.5) of HA has been reported before Ref. [29]. As the electro-spun HA membrane could be dissolved almost instantly in water, we have attempted two post-treatment methods to 'cross-link' the nanofibrous membrane. The first method involved the exposure of electro-spun HA membrane in HCl-vapor. It was found that the HCl-vapor from 37% (w/v) HCl solution could damage the fibrous structure of electro-spun HA membrane in a few minutes, indicating that the decrease in the concentration of HCl solution was necessary. In order to optimize the HCl concentration for treating the electro-spun HA membranes, the partial pressure of HCl as a function of the HCl concentration [33] is shown in Fig. 9. The partial pressure of HCl increases rapidly when the HCl concentration is higher than 30% (w/v). Therefore, for the following experiments, we chose the HCl concentration to be in the range of 20–30% (w/v) in order to provide a milder HCl-vapor treatment.

Fig. 10 shows the SEM images of electro-spun HA membranes treated with HCl-vapor for 3 min (height: 5 cm) using more diluted HCl aqueous solutions at different HCl concentrations: (a) 29%, (b) 24%, (c) 20%, (d) 26% (w/v). The fibers were kept intact and there was no major change in the surface morphology of HA membranes after the HCl-vapor treatment by exposing the membrane at lower HCl-vapor pressures. After the HCl-vapor treatment, the electro-spun HA membranes were kept in sealed bottles and placed in the freezer at −20 °C for weeks.

Fig. 11 shows the SEM images of HA samples treated for different time periods in HCl-vapor and kept in a freezer at −20 °C. With short HCl-vapor exposure times, the membranes could swell in Mill-Q water and become transparent. The swollen HA membranes would not disappear in water for more than one week, but they did become very soft and difficult to pick up from the aqueous fluid. With longer HCl-vapor exposure times, the membrane could keep its shape and did not swell much in the translucent state in Mill-Q water, suggesting a higher degree of cross-linking. However, its mechanical strength remained very weak, as the membrane could break into pieces when being handled. The above results indicate that the cross-linking of electro-spun nanofibrous HA membranes can be performed by HCl-vapor treatment; however, the desired mechanical strength cannot be achieved by this approach.

3.2.2. Treatment by ethanol/HCl/H_2O mixtures

It has been demonstrated that HA could be chemically cross-linked with glutaraldehyde [25] or water-soluble carbodiimide [26] in ethanol or acetone–water mixtures. The organic solvent content in the mixture was at least 65% (v/v) in order to prevent the dissolution of HA. Inspired by this strategy, in the following experiments, we attempted to 'cross-link' the electro-spun HA nanofibrous membrane in acidic ethanol–water mixtures. Three different effects probably take place simultaneously in such mixtures—(1) the presence of sufficient amounts of ethanol would prevent the dissolution of HA in the ethanol/water mixture, (2) the presence of sufficient amounts of HCl would destabilize HA and induce 'cross-linking', and (3) the cooling of the mixture would slow down the reaction. Our results using different treatment conditions can be summarized as follows.

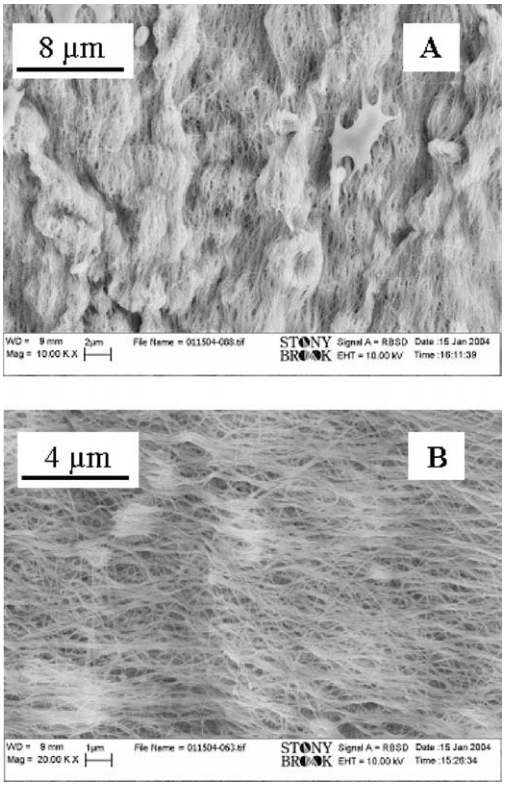

Fig. 12. SEM images of HA membrane soaked in: (A) 3:1 ethanol/HCl mixture for 60 h at 4 °C; (B) 5:1 ethanol/HCl mixture for 1 h, then kept at −20 °C for 60 h.

3.2.2.1. Ethanol/H_2O mixtures at pH 1.5. In our first trial, ethanol/H_2O mixtures at pH = 1.5 were prepared for the post-treatment of electro-spun HA membranes. The volume ratio of ethanol in the mixtures was varied from 65 to 80% (v/v). Three soaking temperatures were selected: −20, 4 and 20 °C. The treatment time was varied from one day to one month. It was found that the fibrous structure of the HA membranes was relatively intact after treatment, but the resulting membranes could be dissolved in neutral water in about 1 s. Thus, the acid content in these mixtures was insufficient, and was increased substantially.

Table 1
Component contents in the ethanol/HCl/H_2O mixture

	(EtOH/37% (w/v) HCl)/H_2O (ml/ml)		
	(3:1) 34/2	(4:1) 16/2	(5:1) 17/2
HCl (% (w/v))	11.7	8.9	7.6
Ethanol (% (v/v))	70.8	71.1	74.6
H_2O (% (v/v))	23.4	24.6	21.8

3.2.2.2. Ethanol/HCl (37%(w/v)) mixtures. In this case, the chosen volume ratios of ethanol and 37% (w/v) HCl were 3:1, 4:1, and 5:1, respectively. The electro-spun HA membranes were immersed into the above ethanol/37% (w/v) HCl mixtures and kept at different temperatures for different time periods. Fig. 12 shows the SEM images of HA membranes soaked in the ethanol/HCl/HA mixture and then kept at different temperatures. In another set of experiments, HA membranes were soaked in the ethanol/HCl mixture, and the membranes were taken out and heated in an oven or a microwave oven for a few minutes (the high temperature treatments were intended to promote the cross-linking process). All samples treated by these very strong acidic ethanol/HCl mixtures showed some degree of cross-linking. The treated membranes could float on the surface of water for several minutes before being immersed into the liquid. The cross-linking of HA membranes was still relatively weak even when treated by such strong acidic ethanol/HCl (37% (w/v)) mixtures. It should be noted that the slightly swollen HA nano-fibers in the non-woven membrane could probably not yet be fully exposed in the strong acid solution. Thus, the cross-linking reaction had not been fully initiated in the interior of those fibers.

3.2.2.3. Ehanol/37% (w/v) HCl/H_2O mixtures. In this set of experiments, extra water was introduced into the ethanol/37% (w/v) HCl mixture. Different ratios of the ethanol/37% (w/v) HCl mixtures (3:1, 4:1, 5:1) were diluted with water. The three component mixture was checked continuously by dropping one small piece of electro-spun HA membrane until the HA membrane changed from complete dissolution to no noticeable shrinkage. The contents of ethanol, H_2O and HCl were then calculated and are summarized in Table 1. The electro-spun HA membranes were immersed into the above three-component mixtures at different temperatures (−20, 4, 20 °C) for different time periods.

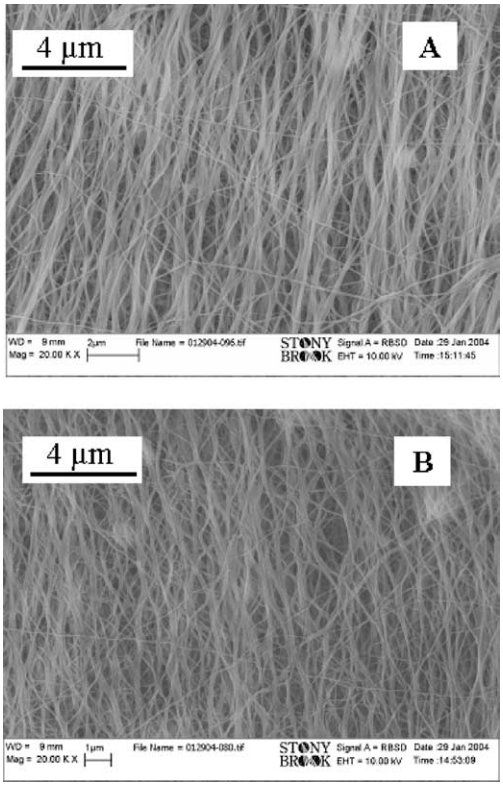

Fig. 13. SEM images of HA membrane treated by: (A) '1-ml H_2O + 17-ml 3:1 ethanol/HCl (37% (w/v))' 4 °C for 16 h; (B) '2-ml H_2O + 16-ml 4:1 ethanol/HCl (37% (w/v))', 4 °C for 20 h.

The resulting membranes under such post-treatment conditions were well cross-linked in the mixture of '3:1 ethanol/HCl + H_2O' and '4:1 ethanol/HCl + H_2O' at 4 °C, as shown in Fig. 13. The cross-linked membrane could keep its shape intact in neutral water for at least 1 week at 25 °C. The cross-linking of samples treated by '5:1 ethanol/HCl + H_2O' mixture at 4 °C was a little weaker, whereby the films became transparent in neutral water. Fig. 14 shows the SEM images of HA membranes treated by 'H_2O + ethanol/HCl' mixture and then soaked in neutral water for different time periods. By treating the samples with H_2O/ethanol/HCl mixture at −20 °C or at 20 °C, the HA membrane would still be dissolved fairly fast in water if the sample was treated in H_2O/ethanol/HCl mixture at −20 °C and for periods even longer than 1 week, indicating that the cross-linking reaction could not occur substantially when the sample was treated in the mixture at low temperatures (e.g. −20 °C). For the sample treated at 20 °C, the mechanical strength of HA membrane was very weak and broke into pieces when soaked in neutral water for several hours, implying that the strong acid would destroy the fibers at higher temperatures (e.g. at 20 °C).

Thus, for the optimal content of ethanol in the mixture, it should be about 71% (v/v). Otherwise, the HA membrane would dissolve or shrink significantly if the ethanol content were a little lower than 71% (v/v). The optimal water content should be about 24% (v/v). If the water content was lower than 23% (v/v), there would not be enough water to ensure the membrane to be sufficiently swollen and the resulting cross-linked HA membranes would be less resistant to water dissolution.

3.3. Probing the possible mechanism of cross-linking HA under acidic conditions

3.3.1. FTIR spectroscopy

To gain some insight into the chemical structure of the cross-linked HA molecules, IR spectroscopy was conducted on the electro-spun membranes before and after cross-linking. The results are shown in Fig. 15 for the HA powder, electro-spun HA membranes before and after treatment in acidic condition. The representative bands can be assigned as follows [34]: the intense group of bands extending from 1500 to 1800 cm^{-1} are super-positions of amides I and II bands and of various carbonyl and carboxyl $\nu_{C=O}$ bands. The bands extending between 950 and 1100 cm^{-1} are

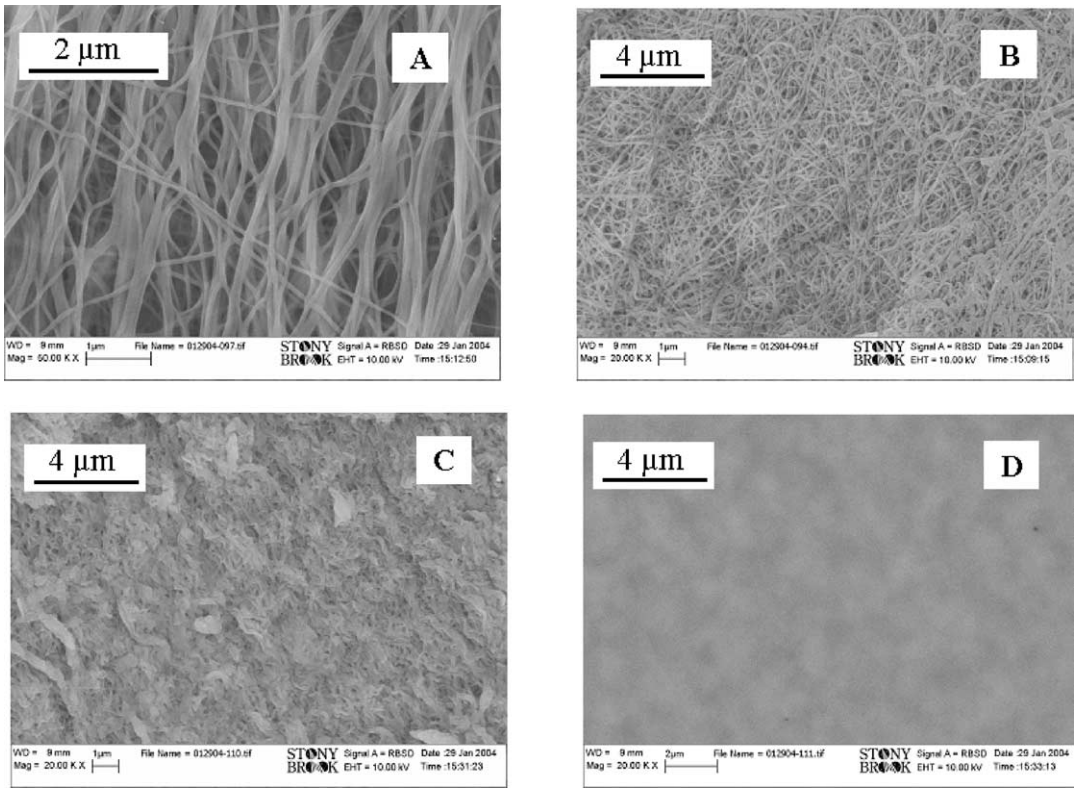

Fig. 14. SEM images of HA membrane treated by '2-ml H_2O + 16-ml 4:1 ethanol/HCl', 4 °C for 20 h: (A) sample dried by filter paper; (B) soaked in water for 5 min; (C) soaked in water for 10 min; (D) soaked in water for 1 day.

mainly resulted from different vibrations of the pyranose ring, corresponding to $\nu_{C–OH}$. The shoulder at 1155 cm^{-1} can be assigned to $\nu_{C–O–C}$. As seen in Fig. 15 (A) and (B), no appreciable difference can be observed in the IR spectra between the virgin powder and the electro-spun HA membrane before treatment, except for the change due to the ion exchange of carboxyl group in HA (from 1600 to 1645 and 1735 cm^{-1}) from $–COO^-Na^+$ to –COOH induced by HCl. Comparing the IR spectra (Fig. 15 (B) and (C)) of electro-spun HA membrane before and after cross-linking under acidic environment, no new peak appeared and no peak shift could be identified. However, the peaks at 1043 and 1078 cm^{-1}, corresponding to $\nu_{C–OH}$, were changed from sharp to blunt. This phenomenon can be attributed to the hydrogen bond of C–OH being strongly enhanced by acid treatment. The results from the IR spectra indicated that the cross-linking of HA in the nanofibrous membrane was probably due to the formation of a hydrogen-bonding network among the chains, leading to an absence of change in the chemical structure, at least from the IR spectroscopic perspective.

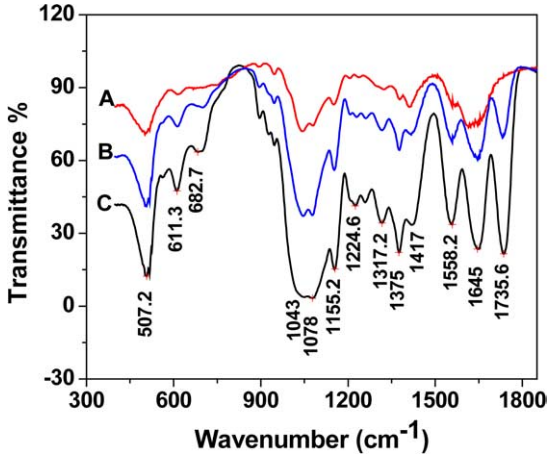

Fig. 15. FTIR spectra of: (A) HA powder; (B) electrospun HA membrane before cross-linking; (C) cross-linked electrospun HA membrane by acidic ethanol/H_2O mixtures.

3.3.2. Viscosity changes of acidic HA aqueous solution after freezing

As reported previously [29], when acidic HA solution was allowed to freeze at −20 °C and was followed by the thawing process, insoluble HA gel could be obtained. In this set of experiments, we attempted to identify the optimal freezing time for acidic HA solution under which the viscosity of HA solution could be increased significantly but in the absence of gel formation. For this purpose, the acidic HA aqueous solution was frozen at −20 °C for different time periods. After freezing, the frozen samples were thawed at room temperature. The final solutions after thawing were transparent, similar to that of the starting solution, if the freezing time was no more than 6 h. However, if

freezing time was longer than 8 h, the final solution after thawing looked like putty, indicating the onset of gel formation. Spongy gels were obtained when the freezing time was longer than 40 h.

As shown in Fig. 16, the shear viscosity of thawed HA solution after freezing for different time periods increased with increasing freezing time from 0 to 6 h. The measured apparent shear viscosity then decreased for the samples frozen for more than 8 h. The reason for this phenomenon was that gel particles began to appear in the HA solution after having been frozen for more than 8 h. The inhomogeneous solution could result in a lower viscosity. Fig. 17 showed the relationship between the extrapolated zero-shear viscosity values of the acidic HA solution and the freezing time. The zero-shear rate viscosity of HA solution increased after a short freezing time period and then decreased with further freezing time. This result indicated that after 6-h of freezing, the acidic HA solution was slightly cross-linked and its viscosity increased significantly with the solution still remaining in a homogeneous solution state. Longer freezing times resulted in the formation of cross-linked HA gel and the occurrence of micro-gel particle formation after thawing.

With the cross-linking reaction occurring in acidic HA solution after a short time period of freezing (less than 6 h), we tried to estimate the molecular weight changes after the freezing process by viscosity measurements. When the thawed solution was neutralized with 0.2 M NaOH solution and then diluted with 0.1 M NaCl solution, the final solution was clear if the freezing time was lower than 6 h. The intrinsic viscosity of diluted HA solution with 0.1 M NaCl before and after 6 h of freezing showed very similar values, as shown in Fig. 18, indicating the reversible nature of this weak cross-linking reaction caused by the freezing process upon dilution.

Fig. 19 shows the shear viscosity of HA solution neutralized with 0.2 M NaOH solution after freezing and thawing processes against the shear rate for two samples frozen at −20 °C for 0 and 6 h, respectively. By comparing the results with those in Fig. 17, it was found that, after neutralization, the viscosity of HA solution remained essentially the same before and after the freezing process,

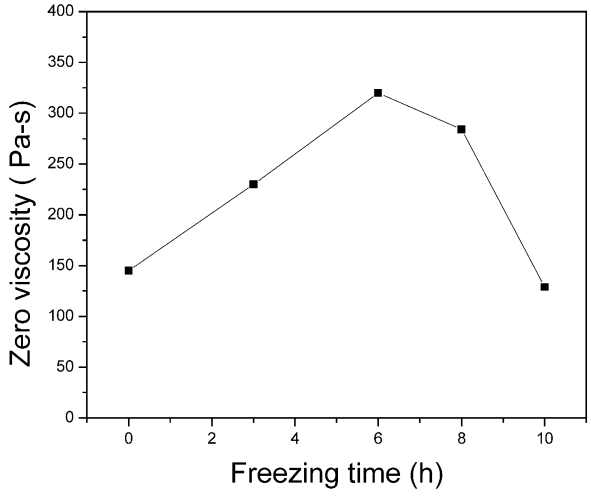

Fig. 17. Extrapolated zero shear viscosity of acidic HA solution versus freezing time.

indicating that the cross-linking of HA solution came from relatively weak interactions, in agreement with the argument of increasing hydrogen bonds. Such a cross-linking reaction is reversible upon neutralization and/or dilution.

4. Conclusions

In this study, the effects of various experimental parameters, including the air-blowing rate, HA concentration, feeding rate of solution, electric field, and type of collectors, on the blowing-assisted electro-spinning performance of hyaluronic acid (HA) were investigated. Scanning electron microscopy (SEM) results revealed that a blowing rate of 70 ft^3/h with the HA concentration range from 2.5 to 2.7% (w/v) formed the optimum conditions for the fabrication of HA nanofibers. Several different types of collectors were compared, which elucidated that the air permeable collector could accelerate the elongation of spinning solution. It was found that there was a strong relationship between the experimental parameters and the diameter of spun nanofibers. As the air-blowing rate was

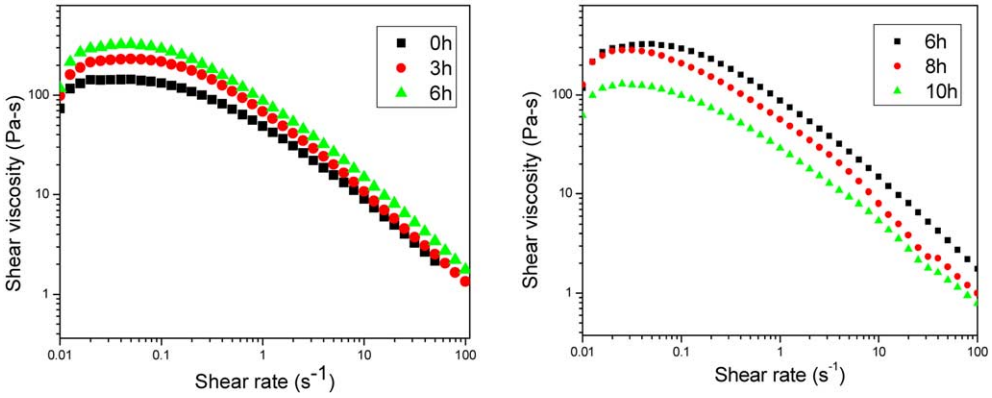

Fig. 16. Effect of freezing time on the shear viscosity of 1.6% (w/v) HA solution (pH 1.5).

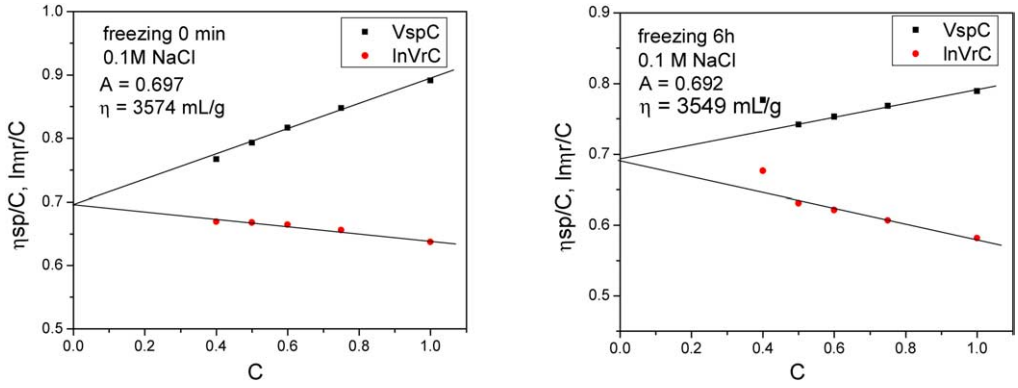

Fig. 18. Relationship between η_{sp}/C, $\ln(\eta_r/C)$ and relative concentration C of dilute HA solutions before and after freezing treatment.

increased to 100 ft^3/h, the fiber diameter was decreased from 87 to 67 nm (above that blowing rate, no further change in the fiber diameter was observed). The concentration also exhibited a linear relationship with the fiber diameter.

The cross-linking of electro-spun HA membranes has been achieved by either the exposure of HCl vapor or by simply immersing the membrane into an ethanol/H_2O/HCl mixture at 4 °C for about 20 h. In the mixture, both the contents of ethanol and of water are very crucial for the successful cross-linking of electro-spun HA membranes. The ethanol content in the mixture should be about 71% (v/v), ensuring that the membrane will not be dissolved or even change its shape significantly. The water content should be about 24% (v/v), ensuring the fibers in the membrane to be slightly swollen to allow the diffusion of HCl into the nanofibers in order for the cross-linking reaction to occur. The cross-linked membrane could keep its shape in neutral water for at least 1 week at 25 °C. The results from IR spectra indicated that the cross-linking of HA in the membrane probably should be attributed to the formation of higher hydrogen-bonding concentration, leading to the formation of the hydrogen-bonded network of the chain.

The cross-linking of acidic HA solution upon freezing was studied by viscosity measurements. The viscosity of HA solution after the freezing-thawing process increased significantly when the freezing time was less than 6 h. However, after neutralization/dilution processes, viscosity measurements showed that the slightly cross-linked HA had almost the same molecular weight as that of the original HA, indicating that the cross-linking of HA solution after freezing for short times was a very weak interaction caused probably by hydrogen bonds, and such a cross-linking reaction could be reversible upon neutralization and/or dilution of the concentrated HA solution. However, the HA solution became gel-like if the freezing time was longer than 8 h, implying that the generation of more hydrogen bonds could form a stronger hydrogen-bonded network. In the current study, we have illustrated that even with the presence of multiple (and often coupled) parameters in the blowing-assisted electro-spinning process, it is feasible to seek a pathway to optimize a specific process and to achieve a reasonable objective.

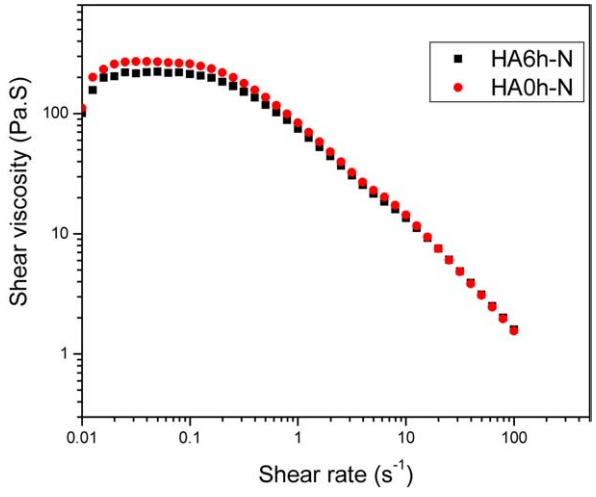

Fig. 19. Shear viscosity of 1.5% (w/v) HA neutralized solution (freezing time: 0 and 6 h).

Acknowledgements

Financial support of this work was provided by NIH-SBIR grants, Phase I (GM63283-02) and Phase II (2R44 GM063283-03A2), and a U.S. Army Research Office (RSECOM) SBIR grant (DAAD16-03-C-0023), administered by Stonybrook Technology and Applied Research, Inc. Dr In Chul Um acknowledges partial support by the Post-doctoral Fellowship Program of the Korea Science and Engineering Foundation (KOSEF).

References

[1] Li WJ, Laurencin CT, Caterson EJ, Tuan TS, Ko FK. J Biomed Mater Res 2002;60:613–21.
[2] Luu YK, Kim K, Hsiao BS, Chu B, Hadjiargyrou M. J Control Release 2003;89:341–53.

[3] Kenawy ER, Layman JM, Watkins JR, Bowlin GL, Matthews JA, Simpson SG, et al. Biomaterials 2003;24:907–13.
[4] Kenawy EF, Abdel-Fattah YR. Macromol Biosci 2002;2:261–6.
[5] Jia H, Zhu G, Vugrinovich B, Kataphinan W, Reneker D, Wang P. Biotechnol Progr 2002;18:1027–32.
[6] Gibson P, Schreuder-Gibson H, Ravin D. Colloid Surf A: Physicochem Eng Aspects 2001;187–8:469–81.
[7] Wang X, Drew C, Lee S, Senecal KJ, Kumar J, Samuelson LA. Nano Lett 2002;2:1273–5.
[8] Yoshimoto H, Shin YM, Terai H, Vacanti JP. Biomaterials 2003;24: 2077–82.
[9] Doshi J, Reneker DH. J Electrostatics 1995;35:151–60.
[10] Fong H, Reneker DH. Polymer 1999;40:4585–92.
[11] Lee KH, Kim HY, La YM, Lee DR, Sung NH. J Polym Sci, Part B: Polym Phys 2002;40:2259–68.
[12] Demir MM, Yilgor I, Yilgor E, Erman B. Polymer 2002;43:3303–9.
[13] Deitzel JM, Kleinmeyer J, Harris D, Tan NCB. Polymer 2001;42: 261–72.
[14] Zong X, Fang D, Kim JS, Kim J, Cruz S, Hsiao BS, et al. Polymer 2002;43:4403–12.
[15] Huang ZM, Zhang YZ, Kotaki M, Ramakrishna S. Compos Sci Technol 2003;63:2223–53.
[16] Balazs EA, Pape LG. Ophthalmology 1980;87:699–705.
[17] Gerke E, Meyer-Schwickerath E, Wessing A. Graefe's Arch Clin Exp Ophthalmol 1984;221:241–3.
[18] Maguen E, Nesburn A, Macy JI. Ophthal Surg 1984;15:55–7.
[19] Folk JC, Weigeist TA, Packer AJ, Howcroft MJ. Ophthal Surg 1986; 17:299–306.
[20] Malson T, Algvere P, Ivert L, Lindqvist B, Selen G, Stenkula S. In: Pizzoferrato A, Marchetti PG, Ravaglioli A, Lee AJC, editors. Biomaterials and clinical applications. Amsterdam: Elsevier Science; 1987. p. 345–8.
[21] Burke S, Sugar J, Farber MD. Ophthal Surg 1999;21:821–6.
[22] Anmarkrud N, Elergaust B, Bulle T. Acta Ophthalmol 1992;70: 96–100.
[23] Um IC, Fang D, Hsiao BS, Okamoto A, Chu B. Biomacromolecules 2004;5(4):1428–36.
[24] Tomihata K, Ikada Y. Biomaterial 1997;18:189–95.
[25] Tomihata K, Ikada Y. J Polym Sci, Part A: Polym Chem 1997;35: 3553–9.
[26] Tomihata K, Ikada Y. J Biomed Res 1997;37:243–51.
[27] Young SC, Sung RH, Young ML, Kang WS, Moon HP, Young SN. J Biomed Res 1999;48:631–9.
[28] Shu XZ, Liu Y, Luo Y, Roberts MC, Prestwich GD. Biomacromolecules 2002;3:1304–11.
[29] Miyata Y, Okamoto A, Kawata M, Oshima K, Hashimoto M, Arai K, et al. United States Patent, US 6387413B1.
[30] Menzies D. Surg Annul 1992;24:27–45.
[31] Zong X, Kim K, Fang D, Ran S, Hsiao BS, Chu B. Polymer 2002;43: 4403–12.
[32] Fridrikh SV, Yu JH, Brenner MP, Rutledge GC. Phys Rev Lett 2003; 90:144502/1–144502/4.
[33] Chemical Safety Data Sheet SD-39. Properties and essential information for safe handling and use of hydrochloric acid, aqueous and hydrogen chloride, anhydrous.: Manufacturing Chemist Association; 1970.
[34] Haxaire K, Marechal Y, Milas M, Rinaudo M. Biopolymers 2003;72: 10–20.